Cell dynamical modelling of vortex dynamics

1991 J. Phys. A: Math. Gen. 24 3323

(http://iopscience.iop.org/0305-4470/24/14/019)

J. Phys. A: Math. Gen. 24 (1991) 3323-3329. Printed in the UK

Cell dynamical modelling of vortex dynamics

Sanjay Puri

School of Physical Sciences, Jawaharlal Nehru University, New Delhi 110067, India

Received 3 December 1990, in final form 18 February 1991

Abstract. We present a computationally efficient, cell dynamical system which mimics the two-component Ginzburg-Landau equation. This model is used to numerically study the time-dependent behaviour of the vorticity number for a two-dimensional lattice. We find that the vorticity number initially decays exponentially in time and subsequently shows a power-law decay in time ($\sim 1/t$, where t is time).

The transition of a system from the normal to the superconducting state is mediated by the formation of vortices and antivortices and their subsequent annihilation. The dynamics of this transition is described by a phenomenological partial differential equation, the two-component time-dependent Ginzburg-Landau (TDGL) equation [1]:

$$\frac{\partial \psi(\boldsymbol{r}, t)}{\partial t} = \tau \psi(\boldsymbol{r}, t) - g|\psi(\boldsymbol{r}, t)|^2 \psi(\boldsymbol{r}, t) + D\nabla^2 \psi(\boldsymbol{r}, t) \tag{1}$$

where $\psi(\boldsymbol{r}, t)$ is a complex order parameter field [$= A(\boldsymbol{r}, t) \exp(i\phi(\boldsymbol{r}, t))$] which depends on space ($\boldsymbol{r}$) and time (t). The coefficients τ, g and D are real and positive and are phenomenological measures of the quench-depth, the coupling strength and the diffusion constant respectively. Typically, (1) describes a system in the normal state which is quenched below the superconducting transition temperature at time $t = 0$. The normal state is characterized by an order parameter field which consists of random fluctuations about a zero background. The dynamics of (1) is characterized by the appearance of vortices and antivortices, which are singularities of the phase field $\phi(\boldsymbol{r}, t)$. (This concept will be elaborated shortly.) More recently, equations similar to (1), but with complex coefficients, have arisen in the study of pattern-forming systems such as amplitude equations ([2] and references therein) and as general models for investigating chaos [3].

The two-component TDGL equation has been the subject of much numerical and analytic work [4]. However, there are no clear numerical results on the time-dependent behaviour of the vorticity/antivorticity or the autocorrelation functions. Loft and DeGrand [5] have performed a Langevin simulation of the planar XY model [6], which is closely related to (1) (C Dasgupta, private communication). Their results indicate that the vorticity/antivorticity number (to be defined shortly) initially decays exponentially in time until a critical vortex density is reached. Subsequently, the vorticity/antivorticity number decays as a power-law in time ($\sim 1/t$). However, their numerical results are not clear, perhaps as a result of the intrinsic limitations of the Langevin simulation technique. In this paper, we present a computationally efficient, cell dynamical system (CDS) model [7-8] which mimics the two-component TDGL equation. We use this model to obtain clear numerical evidence of a crossover in the

0305-4470/91/143323+07$03.50

temporal behaviour of the vorticity/antivorticity number from an 'exponential decay' regime to a 'power-law decay as $1/t$' regime. By an appropriate rescaling of the complex order parameter field $\psi(\boldsymbol{r}, t)$, space $\boldsymbol{r}$ and time t, we can eliminate all the constants in (1). This leads to the dimensionless equation

$$\frac{\partial\psi(\boldsymbol{r}, t)}{\partial t} = \psi(\boldsymbol{r}, t) - |\psi(\boldsymbol{r}, t)|^2\psi(\boldsymbol{r}, t) + \nabla^2\psi(\boldsymbol{r}, t) \tag{2}$$

which is the form we consider in this paper. Oono and Puri [8] have described how computationally efficient CDS models for equations like (2) may be derived. Their scheme involves solving (analytically or numerically) the homogeneous part of (2). The solution of the homogeneous part is then used as the basis of a numerical scheme which is numerically more efficient than the conventional schemes. The enhanced numerical efficiency is a result of the new scheme being numerically stable and reasonable [9], even at high values of the mesh sizes in time and space. To illustrate the application of this scheme to (2), we consider the homogeneous part of (2):

$$\frac{\mathrm{d}\psi(\boldsymbol{r}, t)}{\mathrm{d}t} = \psi(\boldsymbol{r}, t) - |\psi(\boldsymbol{r}, t)|^2\psi(\boldsymbol{r}, t) \tag{3}$$

where $\boldsymbol{r}$ is merely a parameter. Equation (3) is easily solved analytically as

$$\psi(\boldsymbol{r}, t+s) = \frac{\mathrm{e}^s\psi(\boldsymbol{r}, t)}{\sqrt{1+|\psi(\boldsymbol{r}, t)|^2(\mathrm{e}^{2s}-1)}}. \tag{4}$$

Following Oono and Puri [8], this suggests the following computationally efficient scheme for (2):

$$\psi(\boldsymbol{r}, t+\Delta t) = \frac{\mathrm{e}^{\Delta t}\psi(\boldsymbol{r}, t)}{\sqrt{1+|\psi(\boldsymbol{r}, t)|^2(\mathrm{e}^{2\Delta t}-1)}} + \frac{\Delta t}{(\Delta x)^2}\Delta_{\mathrm{D}}\psi(\boldsymbol{r}, t) \tag{5}$$

where $\Delta_{\mathrm{D}}\psi(\boldsymbol{r}, t)$ is the isotropically discretized Laplacian at the point $\boldsymbol{r}$, and Δt, Δx are the size of the time and space increments respectively. A similar scheme has been used by Bohr *et al* [10] to study the onset of defect-mediated turbulence in systems similar to (1), but with complex coefficients. We do not use the scheme (5) but rather an even more efficient scheme which utilizes a local mapping which is piecewise linear and gives a more rapid relaxation to the local fixed points. Thus, we use the scheme

$$\psi(\boldsymbol{r}, t+1) = f(\psi(\boldsymbol{r}, t)) + \alpha\Delta_{\mathrm{D}}\psi(\boldsymbol{r}, t) \tag{6}$$

where the time t is incremented in discrete steps, in the spirit of cell dynamical modelling [7]. In (6), the function $f(x)$ has the form

$$f(x) = \begin{cases} Ax & \text{for } |x| \leqslant 1/A \\ x/|x| & \text{for } |x| > 1/A \end{cases} \tag{7}$$

and A and α are arbitrary parameters (α may be considered to be the counterpart of $\Delta t/(\Delta x)^2$ in (5)). For appropriately chosen values of the parameters A and α, this scheme enables an accelerated access to the asymptotic regime and is in the same dynamical universality class as (5). For the one-component TDGL equation, we have numerically demonstrated this in previous papers [8]. We have confirmed this numerically for the two-component TDGL equation also. With an appropriate rescaling of time, the results obtained from (5) are identical to those obtained from (6). Thus, we present here only results obtained from (6). As already mentioned, the difference

between the time scales of (5) and (6) is a result of the difference in the local mapping of the two schemes. The local mapping in both the schemes has an unstable fixed point (at $\psi(r, t) = 0$) and a circle of stable fixed points (at $|\psi(r, t)| = 1$), giving rise to similar dynamics. However, the local mapping of (6) relaxes to the fixed points considerably more rapidly than the local mapping of (5). Hence, the scheme (6) enables us to access the asymptotic regime more rapidly. The parameters A and α should be chosen so as to give reasonable numerical results [8]. In this paper, we use the parameter values $A = 1.3$ and $\alpha = 0.5$. If we match the behaviour of the local mappings in (5) and (6) for small values of $\psi(r, t)$, these values of A and α correspond to the mesh sizes $\Delta t \approx 0.262$ and $\Delta x \approx 0.724$ in the new scheme (5). For the conventional schemes (e.g. explicit discretization scheme), these mesh sizes are unreasonably large for the simulation of (2).

We have implemented (6) on a square lattice with periodic boundary conditions. Figure 1 shows the evolution of a 40×40 lattice from an initial condition consisting of random fluctuations of maximum amplitude 0.05 (and random phase) about a zero background. The configurations are labelled by the number of update steps (subsequently referred to as 'time') which they correspond to and are drawn as follows.

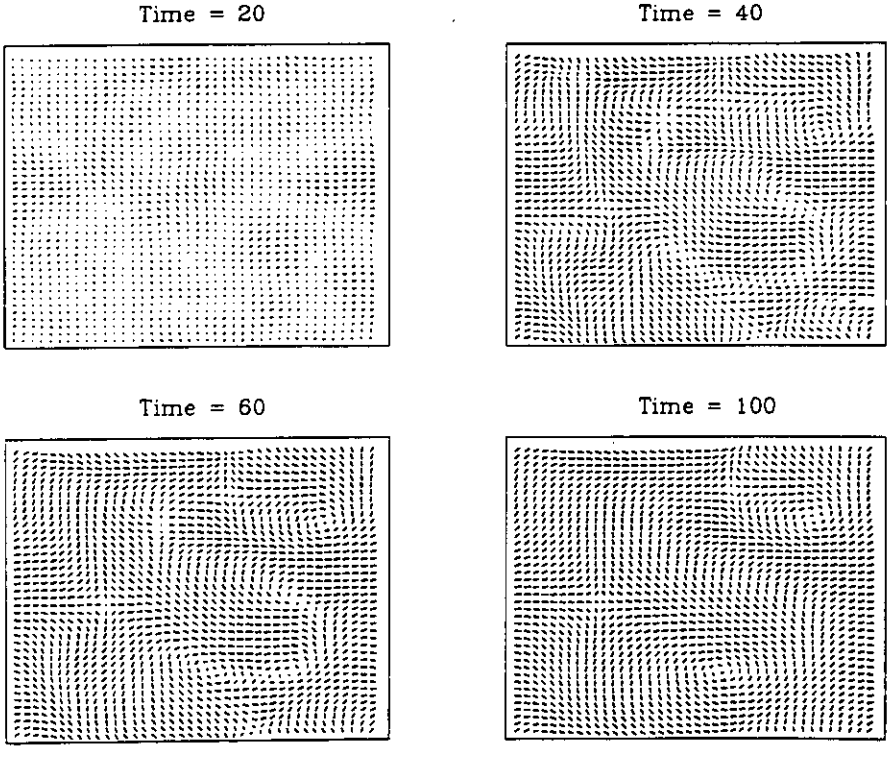

Figure 1. Temporal evolution of our cell dynamical model for a 40×40 lattice. The initial condition (time = 0) consists of random fluctuations of maximum amplitude 0.05 (and random phase) about a zero background. At each point of the lattice, we draw a line whose length is proportional to the amplitude of the complex order parameter at that point. This line is inclined to the positive x-direction at an angle equal to the phase of the complex order parameter. The 'time' which labels each configuration refers to the number of update steps from the initial condition.

At each point of the lattice, we draw a line whose length is proportional to the amplitude $A(r, t)$ of the complex order parameter field $\psi(r, t)$. This line is inclined to the positive x-direction at an angle corresponding to the phase $\phi(r, t)$ of the complex order parameter field. As mentioned earlier, vortices and antivortices constitute singularities of the phase field. Thus, the total variation of the phase field around a closed loop (viz, $\Delta\phi = \oint d\phi$) is non-zero if the loop encloses vortices or antivortices. The vorticity or antivorticity number is the integer part of $\Delta\phi/(2\pi)$, say n. If n is positive (negative), the closed loop is said to include a vortex (antivortex). In figure 1, the earlier configurations (e.g. the picture at 20 update steps) consists of a large number of vortices and antivortices which annihilate each other through a variety of mechanisms. This gives rise to a dilute gas of vortices and antivortices (e.g. the picture at 100 update steps). Because of finite-size effects, the ultimate configuration of this lattice (not shown in figure 1) corresponds to a spatially uniform complex order parameter field, with an amplitude of 1 and a constant phase angle which depends on the initial condition chosen. This is unphysical as the thermodynamic ground state of this system corresponds to a diffuse gas of vortices and antivortices [5, 6]. For larger lattices, the (unphysical) uniform state is accessed at later times, as expected. Figure 2 shows the variation of the real and imaginary components of the complex order parameter field

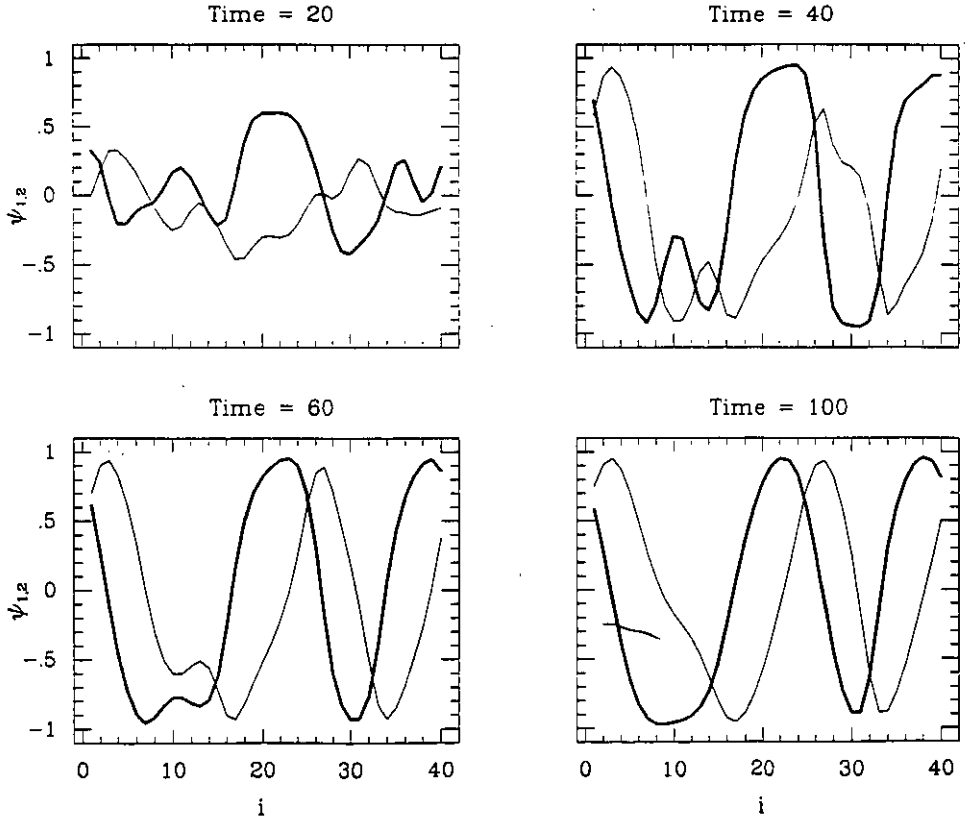

Figure 2. Variation of the real and imaginary components of the complex order parameter along a diagonal section ($i = j$) of figure 1. The real component ($\psi_1(r, t)$) is denoted by a heavy line and the imaginary component ($\psi_2(r, t)$) is denoted by a light line.

along the diagonal ($i=j$) of the 40×40 lattice for the configurations shown in figure 1. The real component ($\psi_1(r,t)=\mathrm{Re}[\psi(r,t)]$) is denoted by a heavy line and the imaginary component ($\psi_2(r,t)=\mathrm{Im}[\psi(r,t)]$) is denoted by a light line. This indicates the rapidity ($t\approx40$) with which the amplitude saturates out to the equilibrium value of 1.

To study the time evolution of the vorticity number of the lattice, we use the definition of vorticity number given by Tobochnik and Chester [11]. Vortices and antivortices are considered to live on a 1×1 square. To compute the vorticity number associated with a particular 1×1 square, we start off at one of the corners of the square and traverse the corners in a clockwise direction. The net change of the phase angle around the square is the sum of phase angle differences (defined to lie between $-\pi$ and π) between the complex order parameter field at successive corners of the square. As stated earlier, the vorticity number or antivorticity number associated with the 1×1 square is the integer part of the net change of the phase angle divided by 2π. The net vorticity number (antivorticity number) of the lattice is the sum of the vorticity numbers (antivorticity numbers) associated with each square. Figure 3 shows the time-dependence of the vorticity number (N_v) for a 100×100 lattice. The data shown in figure 3 was obtained as an average over 20 runs from different initial conditions, each consisting of random fluctuations of maximum amplitude 0.05 (and random phase) about a zero

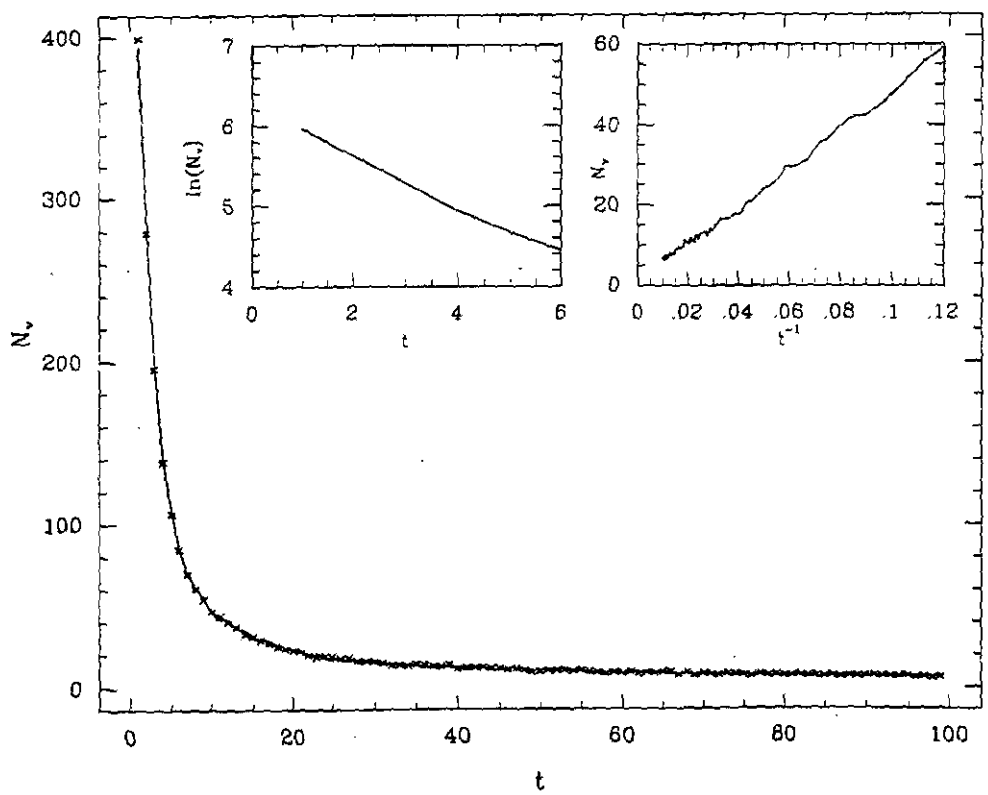

Figure 3. Time dependence of the vorticity number N_v (defined in the text) for a 100×100 lattice. The data is computed as an average over 20 different initial conditions of the type used in figure 1. The left inset figure shows $\ln(N_v)$ versus t for earlier times ($\lesssim6$) and the right inset figure shows N_v versus t^{-1} for later times ($\gtrsim8$).

background. The solid line in the main figure shows N_v as a function of time t. The crosses show the temporal behaviour of the antivorticity number as a function of time. This data is superposed on the main figure to show that, within statistical fluctuations, the vorticity and antivorticity numbers are the same. The inset figures show the temporal dependence of N_v for earlier times (left inset) and later times (right inset). For earlier times (≤ 6), we plot $\ln(N_v)$ versus t in the left inset figure, showing that the vorticity number initially decays exponentially in time. This is the result of vortex-antivortex annihilation at a rate proportional to the number of vortex-antivortex pairs [5]. For later times (≥ 15), the system is dominated by isolated vortices and antivortices which annihilate through Brownian diffusion [5], giving rise to a power-law decay as $N_v \sim 1/t$. This is shown in the right inset figure, where we plot N_v versus $1/t$.

At this stage, a general remark about the errors involved in these calculations is in order. The dynamics is deterministic so the only source of errors is numerical inaccuracy. All our calculations were performed in the double precision mode. Furthermore, the dynamics is always attractive (to stable fixed points). Thus, we do not expect large errors in these calculations.

To summarize: we have presented a simple cell dynamical model which mimics the two-component TDGL equation (2). This model is easily implemented numerically and gives a rapid evolution from an arbitrary initial condition. We have used this model to obtain unambiguous numerical results on the temporal behaviour of the vorticity number. These results show a quick crossover from an initial 'exponential decay' regime to a subsequent 'power-law decay as $1/t$' regime.

Acknowledgments

The author is grateful to R C Desai for inviting him to spend the summer of 1990 at the Department of Physics, University of Toronto, where the numerical work described in this text was performed. The idea for this cell dynamical model was conceived during conversations with Y Marathe and S Sengupta. The author also enjoyed useful conversations with C Dasgupta.

References

[1] Ginzburg V L and Landau L D 1950 *Zh. Eksp. Teor. Fiz.* **20** 1064
Hohenberg P C and Halperin B I 1977 *Rev. Mod. Phys.* **49** 435
[2] Sirovich L, Rodrigues J D and Knight B 1989 *Physica* **43D** 63
Rodrigues J D and Sirovich L 1989 *Physica* **43D** 77
[3] Moon H T, Huerre P and Redekopp L G 1982 *Phys. Rev. Lett.* **49** 7
[4] Mazenko G F and Zannetti M 1985 *Phys. Rev.* B **32** 4565
Toyoki H and Honda K 1986 *Prog. Theor. Phys.* **78** 273
Mondello M and Goldenfeld N 1990 *Phys. Rev.* A **42** 5865
[5] Loft R and DeGrand T A 1987 *Phys. Rev.* B **35** 8528
[6] Kosterlitz J M 1982 *Nonlinear Phenomena at Phase Transitions and Instabilities* ed T Riste (New York: Plenum) and references therein
[7] Wolfram S 1986 *Theory and Applications of Cellular Automata* (Singapore: World Scientific)
Kaneko K 1984 *Prog. Theor. Phys.* **72** 480
Kapral R 1985 *Phys. Rev.* A **32** 1076
Oppo G L and Kapral R 1986 *Phys. Rev.* A **33** 4219

[8] Oono Y and Puri S 1987 *Phys. Rev. Lett.* **58** 836
Oono Y and Puri S 1984 *Phys. Rev.* A **38** 434
Puri S and Oono Y 1988 *Phys. Rev.* A **38** 1542
[9] Parekh N and Puri S 1990 *J. Phys. A: Math. Gen.* **23** L1085
[10] Bohr T, Pedersen A W, Jensen M H and Rand D A 1989 *New Trends in Nonlinear Dynamics and Pattern Forming Processes* ed P Coullet and P Heurre (New York: Plenum)
[11] Tobochnik J and Chester G V 1979 *Phys. Rev.* B **20** 3761